

Northumbria Research Link

Citation: Mann, Paul, Spencer, Robert, Dinga, Bienvenu, Poulsen, John, Hernes, Peter, Fiske, Greg, Salter, Matthew, Wang, Zhaohui, Hoering, Katherine, Six, Johan and Holmes, Robert (2014) The biogeochemistry of carbon across a gradient of streams and rivers within the Congo Basin. *Journal of Geophysical Research Biogeosciences*, 119 (4). pp. 687-702. ISSN 2169-8961

Published by: Wiley-Blackwell

URL: <http://dx.doi.org/10.1002/2013JG002442> <<http://dx.doi.org/10.1002/2013JG002442>>

This version was downloaded from Northumbria Research Link:
<http://nrl.northumbria.ac.uk/16030/>

Northumbria University has developed Northumbria Research Link (NRL) to enable users to access the University's research output. Copyright © and moral rights for items on NRL are retained by the individual author(s) and/or other copyright owners. Single copies of full items can be reproduced, displayed or performed, and given to third parties in any format or medium for personal research or study, educational, or not-for-profit purposes without prior permission or charge, provided the authors, title and full bibliographic details are given, as well as a hyperlink and/or URL to the original metadata page. The content must not be changed in any way. Full items must not be sold commercially in any format or medium without formal permission of the copyright holder. The full policy is available online: <http://nrl.northumbria.ac.uk/policies.html>

This document may differ from the final, published version of the research and has been made available online in accordance with publisher policies. To read and/or cite from the published version of the research, please visit the publisher's website (a subscription may be required.)

www.northumbria.ac.uk/nrl



RESEARCH ARTICLE

10.1002/2013JG002442

Key Points:

- Vegetation cover predominately controls fluvial C concentration and composition
- Small streams (20 m wide) and wetlands are significant sources of aquatic CO₂
- Changing vegetation cover, or hydrologic conditions impact regional carbon budgets

Supporting Information:

- Readme
- Table S1

Correspondence to:

P. J. Mann,
paul.mann@northumbria.ac.uk

Citation:

Mann, P. J., et al. (2014), The biogeochemistry of carbon across a gradient of streams and rivers within the Congo Basin, *J. Geophys. Res. Biogeosci.*, 119, doi:10.1002/2013JG002442.

Received 2 JUL 2013

Accepted 22 MAR 2014

Accepted article online 28 MAR 2014

The biogeochemistry of carbon across a gradient of streams and rivers within the Congo Basin

P. J. Mann^{1,2}, R. G. M. Spencer¹, B. J. Dinga³, J. R. Poulsen⁴, P. J. Hernes⁵, G. Fiske¹, M. E. Salter⁶, Z. A. Wang⁷, K. A. Hoering⁷, J. Six⁸, and R. M. Holmes¹

¹Woods Hole Research Center, Falmouth, Massachusetts, USA, ²Department of Geography, Northumbria University, Newcastle Upon Tyne, UK, ³Groupe de Recherche en Sciences Exactes et Naturelles (GRSEN), Délégation Générale à la Recherche Scientifique et Technologique (DGRST), Brazzaville, Republic of Congo, ⁴Nicholas School of the Environment, Duke University, Durham, North Carolina, USA, ⁵Department of Land, Air and Water Resources, University of California, Davis, California, USA, ⁶Department of Applied Environmental Science, Stockholm University, Stockholm, Sweden, ⁷Department of Marine Chemistry and Geochemistry, Woods Hole Oceanographic Institution, Woods Hole, Massachusetts, USA, ⁸Department of Environmental Systems Science, ETH-Zürich, Zürich, Switzerland

Abstract Dissolved organic carbon (DOC) and inorganic carbon (DIC, $p\text{CO}_2$), lignin biomarkers, and theoretical properties of dissolved organic matter (DOM) were measured in a gradient of streams and rivers within the Congo Basin, with the aim of examining how vegetation cover and hydrology influences the composition and concentration of fluvial carbon (C). Three sampling campaigns (February 2010, November 2010, and August 2011) spanning 56 sites are compared by subbasin watershed land cover type (savannah, tropical forest, and swamp) and hydrologic regime (high, intermediate, and low). Land cover properties predominately controlled the amount and quality of DOC, chromophoric DOM (CDOM) and lignin phenol concentrations (Σ_g) exported in streams and rivers throughout the Congo Basin. Higher DIC concentrations and changing DOM composition (lower molecular weight, less aromatic C) during periods of low hydrologic flow indicated shifting rapid overland supply pathways in wet conditions to deeper groundwater inputs during drier periods. Lower DOC concentrations in forest and swamp subbasins were apparent with increasing catchment area, indicating enhanced DOC loss with extended water residence time. Surface water $p\text{CO}_2$ in savannah and tropical forest catchments ranged between 2,600 and 11,922 μatm , with swamp regions exhibiting extremely high $p\text{CO}_2$ (10,598–15,802 μatm), highlighting their potential as significant pathways for water-air efflux. Our data suggest that the quantity and quality of DOM exported to streams and rivers are largely driven by terrestrial ecosystem structure and that anthropogenic land use or climate change may impact fluvial C composition and reactivity, with ramifications for regional C budgets and future climate scenarios.

1. Introduction

Fluvial systems are increasingly recognized as important components of the global carbon (C) cycle, acting as both significant transporters of C offshore as well as sites of active heterotrophic metabolism, resulting in the return of greenhouse gases to the atmosphere [Aufdenkampe et al., 2011; Battin et al., 2009; Cole et al., 2007]. The amount and quality (composition) of C and its associated dissolved organic matter (DOM) pool, supplied to fluvial systems from land may be influenced by a variety of factors including climate, catchment vegetation cover and land use [Hood and Scott, 2008; Wilson and Xenopoulos, 2008; Yamashita et al., 2011]. DOM plays a multifaceted role in freshwaters, including light attenuation, trace metal transport and acid-base chemistry [Aiken et al., 2011; Del Vecchio and Blough, 2004; Wang et al., 2013]. Thus, any natural or anthropogenic-driven change that alters exported DOM composition also influences biogeochemical cycling and the structure of downstream aquatic food webs. Despite the critical link among terrestrial ecosystem structure, climate and the composition of C in fluvial environments, only a limited number of studies have attempted to quantify how subbasin-scale land cover properties affect aquatic DOM export and quality [Wilson and Xenopoulos, 2008; Yamashita et al., 2011].

Tropical river systems supply ~60% of global terrigenous dissolved organic carbon (DOC) flux to the ocean [Aitkenhead and McDowell, 2000; Mayorga et al., 2010], yet with the exception of the Amazon Basin, have historically received far less attention compared to their temperate and northern high-latitude counterparts.

The Congo River Basin is the second largest river system on Earth based upon freshwater discharge ($\sim 45,000 \text{ m}^3 \text{ s}^{-1}$) and total drainage basin size ($\sim 3.7 \times 10^6 \text{ km}^2$) but has had limited study with respect to its role in regional-scale C budgets [Coynel *et al.*, 2005; Laraque *et al.*, 2009; Spencer *et al.*, 2012a]. The Congo River is estimated to export approximately 12.4 Tg of DOC, making it the second largest exporter of DOC to the ocean after the Amazon River [Coynel *et al.*, 2005]. Tropical freshwater systems often support high rates of heterotrophic respiration causing elevated rates of carbon dioxide (CO_2) outgassing relative to temperate and boreal systems [Aufdenkampe *et al.*, 2011] and in situ losses of DOC during water transit through a catchment [Worrall *et al.*, 2012]. The Amazon River, for example, has been estimated to return $\sim 500 \text{ Tg C yr}^{-1}$ to the atmosphere roughly equaling the total terrestrial sequestration in vegetation across the entire Amazon Basin [Richey *et al.*, 2009]. A large proportion of the CO_2 originating from the Amazon derives from in situ respiration of terrigenous C [Mayorga *et al.*, 2005]. Thus, CO_2 evasion from fluvial networks within large tropical watersheds represents a missing sink for terrestrial organic C that is not captured when solely examining riverine land to ocean flux estimates.

Current conditions in the Congo Basin present a unique opportunity to understand controls upon the biogeochemistry of carbon in a pristine major tropical river system. The Congo Basin hosts the Earth's second largest tropical rainforest, vast areas of savannah and extensive regions of swamp forest and wetlands covering at least $> 65,000 \text{ km}^2$ that undergo permanent and seasonal inundation [Bwangoy *et al.*, 2010]. In common with the majority of tropical regions, the Congo Basin is facing ever increasing regional and global challenges associated with climate change (e.g., increasing temperatures and altered precipitation patterns), as well as local land use changes such as deforestation and major dam construction [Aerts *et al.*, 2006; Koenig, 2008; Spencer *et al.*, 2014]. Thus, understanding DOM transport and C cycling dynamics within these regions, and how inland water chemistry may change in relation to catchment characteristics, will enable us to make improved predictions of watershed C budget alterations under future land use and climate scenarios. Further, it is imperative that we gain a better understanding of how these systems currently function, as they represent unique environments yet to be impacted by significant anthropogenic change allowing us to adequately construct a baseline for comparison to future perturbations.

The main objectives of this study were (1) to identify the role of land cover and hydrology in controlling the quantity and character of DOM exported from subbasins across the Congo River Basin, (2) to examine CO_2 measurements in freshwaters, especially in currently understudied small stream ($< 5\text{--}10 \text{ m}$ width) and swamp environments that are disproportionately important with respect to CO_2 outgassing, and (3) to examine the use of optical properties as proxies for molecular measurements. Objectives one and two are critical for assessing the impacts that future shifts in land cover and hydrology will have on land to ocean export and water-air efflux of C. Objective three is of great interest given that optical measurements can now be undertaken via in situ technologies. Proper calibration may provide leveraging to obtain high temporal and spatial resolution of DOM quality that are required to actually understand DOM dynamics in freshwater environments [Hernes *et al.*, 2009; Pellerin *et al.*, 2011; Spencer *et al.*, 2012b].

2. Methods

2.1. Study Site

Samples were collected during 2010 and 2011 predominantly from sites within the Republic of Congo, in the northwest region of the Congo River Basin (Figure 1 and Table S1 in the supporting information). In total, three synoptic sampling trips were conducted, visiting 56 separate sites. Twenty of these sites were measured on all three sampling trips (February 2010, November 2010, and August 2011). Due to logistical constraints, it was not possible to visit all of the same sites on each of the sampling trips. Sample sites were selected to cover a gradient of land vegetation cover (see section 2.3), and waters of each type were sampled during each trip.

As our sites straddled the equator, the stage of the hydrograph at each stream or river varied not only with sample date but also by region. The hydrologic regime at each site was therefore classified via stage height as high, intermediate, or low using recent or historic discharge data. When hydrologic data were unavailable for a site, the discharge state was categorized using precipitation data from the nearest weather station. The discharge and precipitation data were obtained from the Groupe de Recherche en Sciences Exactes et Naturelles in the Republic of Congo, with support from the Institute of Research for Development

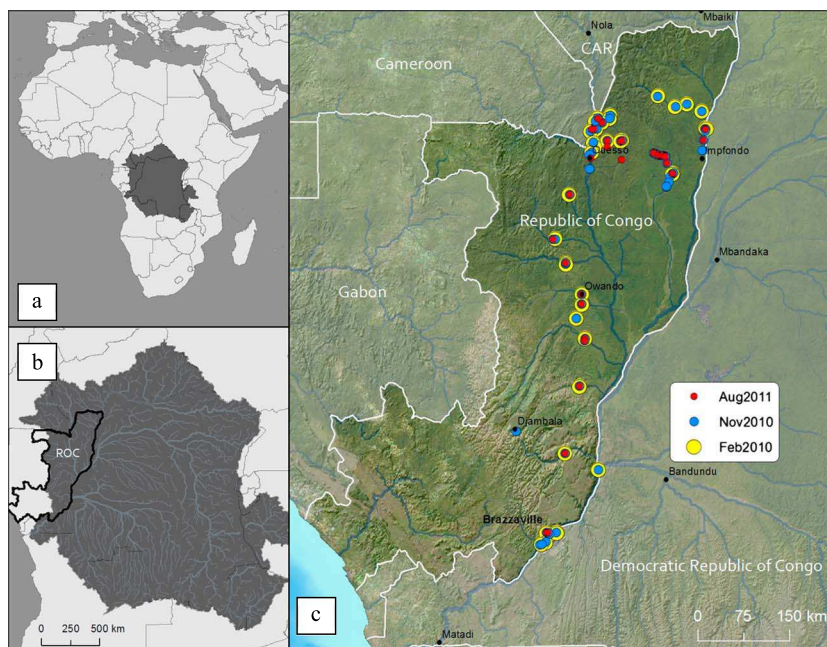


Figure 1. Map of study sites. (a) The grey shading represents the Congo River Basin, (b) the Republic of Congo where the majority of samples were collected. (c) Inset shows individual study sites and sample dates.

in France [ORSTOM, 1979]. Hydrologic regimes assessed using precipitation data from stations close to streams with concurrent discharge stage height records were identical, suggesting this was a viable method for assessing hydrologic regime in ungauged areas.

2.2. Sample Collection

Samples were collected from the thalweg of the stream or river using a peristaltic pump with tubing lowered to a depth of ~30 cm. Stream or river pH, conductivity, water temperature, and dissolved oxygen concentrations were collected using a precalibrated handheld instrument (YSI Pro-Plus) at all sites.

Samples for DOC, total dissolved nitrogen (TDN), inorganic nutrients (NH_4^+ , $\text{NO}_3^-/\text{NO}_2^-$), and DOM optical characterization were collected at each site, on all occasions. Sample waters were filtered on site through precombusted (4 h, 550°C) glass fiber filters (nominal pore size 0.7 μm Whatman GF/F) into acid precleaned and triple filtrate-rinsed HDPE plastic bottles. Samples for DOC, TDN, and nutrients were subsequently acidified to pH <2 using trace metal grade hydrochloric acid. Samples for optical analyses were filtered as above but left unacidified and typically run within 2 weeks of collection. At selected sites, additional samples for lignin phenol analysis were collected during two of the sampling trips (February and November 2010). One liter acid precleaned HDPE bottles were filled on site after filtration through in-line capsule filters (Gelman AquaPrep 0.45 μm) and acidified with HCl to pH <2. Finally, samples for dissolved inorganic carbon (DIC) and total alkalinity (TA) were also collected during the November 2010 sampling trip. Discrete DIC and TA samples were independently filtered through capsule filters (Gelman AquaPrep 0.45 μm) into 250 ml borosilicate glass bottles ensuring minimum air contact. Samples were poisoned with HgCl_2 and grease sealed with ground glass stoppers for storage. All samples were kept dark and chilled until refrigeration upon return to a local laboratory. All preserved samples were run within 2 months of collection.

2.3. Dominant Land Cover Classification

Sample site locations were georeferenced to the World Geodetic System and intersected with the highest-level subwatershed polygons defined by the HYDRO1K global hydrologic data set [U.S. Geological Survey, 2000]. For each site, total area of the contributing watershed was calculated in a geographic information system (GIS) (Table S1 in the supporting information). The fractional land cover type of the contributing watershed region was calculated as per the Global Land Cover (GLC) 2000 data set and binned into one of three distinct land cover categories: (1) Savannah catchments containing grass and low-level shrub classes,

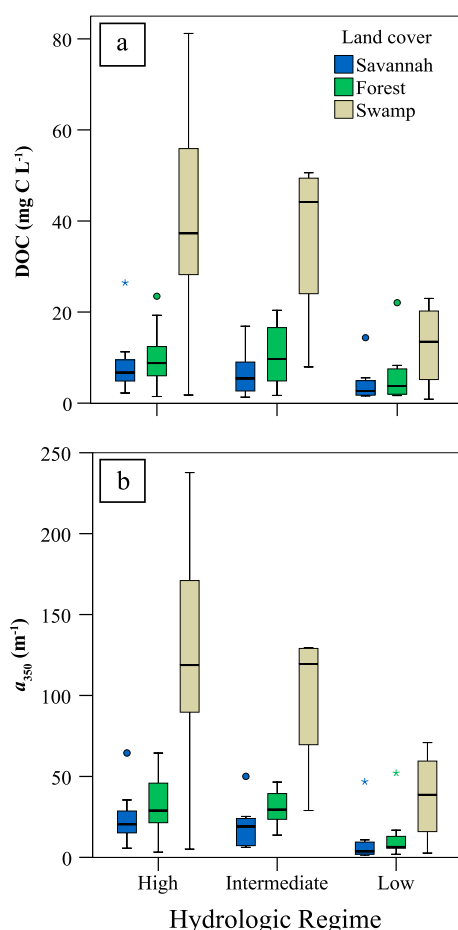


Figure 2. Boxplots of (a) DOC and (b) a_{350} during high, intermediate, and low hydrologic conditions within each of the three land cover types (savannah, forest, and swamp). The black line within each box represents the mean, the height of each box denotes the 25th and 75th percentiles, and the error bars denote the 10th and 90th percentiles.

CDOM source and transformations in a wide range of natural waters [Helms *et al.*, 2008; Spencer *et al.*, 2012b]. S_R values often correlate with DOM molecular weight, increases in the ratio representing decreasing mean DOM molecular weight [Helms *et al.*, 2008; O'Donnell *et al.*, 2010]. The specific UV absorbance at 254 nm ($SUVA_{254}$) was calculated by normalizing the decadal spectrophotometer absorbance (A) to DOC concentration and is presented in units of $L\ mg\ C^{-1}\ m^{-1}$. $SUVA_{254}$ measurements positively correlate with DOM aromaticity, with higher values indicating the presence of more complex aromatic moieties [Weishaar *et al.*, 2003].

CDOM fluorescence was measured using a Horiba Fluoromax 4 spectrofluorometer. The fluorescence index (FI) was calculated as the ratio of the corrected fluorescence emission intensity at 470 and 520 nm, after excitation at 370 nm [Cory and McKnight, 2005; McKnight *et al.*, 2001]. FI values vary with DOM aromaticity [Spencer *et al.*, 2010a] and are commonly used as an indicator of terrestrial/higher plant (FI values ~ 1.3) versus aquatic/microbial-derived CDOM sources (values > 1.5) [Cory and McKnight, 2005].

2.6. Lignin Phenol Analysis

Lignin phenols were measured via the CuO oxidation method described by Hedges and Ertel [1982], with modifications as outlined by Spencer *et al.* [2010b]. In brief, filtered whole waters were acidified to pH 2 with 12 N HCl, rotary evaporated to ~ 3 mL, transferred to Monel reaction vessels (Prime Focus, Inc.) and dried under vacuum centrifugation. All samples were alkaline oxidized at 155°C in a stoichiometric excess of CuO,

(2) tropical forest comprised of both mixed and mosaic forest types, and (3) seasonally inundated or continually flooded swamp forest regions. These land cover categories are referred to throughout the remainder of the manuscript as savannah, forest, or swamp.

2.4. DOC, TDN, and DON Analyses

DOC and TDN were measured via high-temperature catalytic oxidation on a Shimadzu TOC/TN-V instrument combined with a nitrogen chemiluminescence detection unit (TNM-1). DOC concentration is reported as the mean of three to five replicate injections where the coefficient of variation was $< 2\%$ [Mann *et al.*, 2012]. Inorganic nutrients (NO_3^-/NO_2^- and NH_4^+) were measured on an Astoria autoanalyzer using established methods [U.S. Environmental Protection Agency, 1984]. DON concentration was calculated by subtracting the sum of inorganic N from TDN measurements. DOM C:N ratios were determined as the molar ratio of DOC to DON.

2.5. CDOM Optical Analysis

CDOM absorbance measurements were collected on a Shimadzu UV1800 dual-beam spectrophotometer using 10 mm path length quartz cuvettes. All measurements were run in triplicate and referenced against $18.2\ M\Omega\ cm^{-1}$ Milli-Q laboratory water. Absorbance coefficients were calculated as $a_\lambda = 2.303A(\lambda) / l$, where A is the raw absorbance from the spectrophotometer, a the Napierian absorbance coefficient (m^{-1}) at wavelength (λ), and l the cell path length in meters. The spectral slope (S) was calculated using a nonlinear fit to the exponential function of the absorbance spectrum. Spectral slopes were calculated over two wavelength ranges spanning 275 to 295 ($S_{275-295}$) and 350 to 400 nm ($S_{350-400}$). The spectral slope ratio (S_R) was then calculated as the ratio of the two ($S_{275-295} / S_{350-400}$) [Helms *et al.*, 2008]. These spectral slope ranges and ratios have been identified as particularly sensitive indicators of

Table 1. DOC Concentration, C:N Ratios and CDOM Quantity (a_{350}), and Optical Quality Parameters ($S_{275-295}$, $S_{350-400}$, S_R , FI and SUVA₂₅₄)^a

	DOC (mg C L ⁻¹)			C:N (Molar)			a_{350} (m ⁻¹)			$S_{275-295}$ (x10 ³ nm ⁻¹)			$S_{350-400}$ (x10 ³ nm ⁻¹)			Slope Ratio (S_R)			Fluorescence Index (FI)			SUVA ₂₅₄ (L mg C ⁻¹ m ⁻¹)			
	Mean	Max	Min	Mean	Max	Min	Mean	Max	Min	Mean	Max	Min	Mean	Max	Min	Mean	Max	Min	Mean	Max	Min	Mean	Max	Min	
High																									
Savannah	9.2	26.4	2.2	37.3	51.0	30.0	25.5	64.5	5.7	12.44	13.29	11.45	16.04	17.66	11.90	0.79	1.00	0.73	1.27	1.35	1.15	4.2	4.7	3.4	
Forest	10.1	23.5	1.5	30.8	40.5	25.4	31.7	64.4	3.2	12.12	13.27	10.19	15.81	17.89	8.75	0.79	1.19	0.71	1.72	1.35	1.23	4.5	5.8	2.3	
Swamp	41.2	81.2	1.8	46.2	57.6	18.6	123.9	237.7	5.1	12.58	12.87	11.47	17.78	18.75	14.72	0.71	0.78	0.68	1.20	1.32	1.13	4.3	4.6	3.3	
Intermediate																									
Savannah	6.1	16.9	1.3	26.2	35.5	18.9	18.8	50.0	6.2	12.76	14.66	11.44	16.88	18.15	15.91	0.76	0.87	0.71	1.38	1.38	1.25	5.0	5.9	4.1	
Forest	10.6	20.4	1.7	26.8	32.8	17.3	30.3	46.5	13.7	12.76	15.61	11.84	16.57	17.36	15.57	0.77	1.00	0.71	1.25	1.35	1.22	4.4	5.2	2.7	
Swamp	36.7	50.6	7.9	-	-	-	99.3	129.5	29.0	12.91	13.09	12.78	18.03	18.66	16.61	0.72	0.77	0.70	1.20	1.24	1.17	4.7	5.3	4.5	
Low																									
Savannah	4.3	14.4	1.6	31.4	42.6	20.2	9.8	46.8	1.5	19.56	30.62	11.81	16.24	17.05	14.93	1.20	1.88	0.74	1.36	1.48	1.27	3.0	5.5	1.8	
Forest	6.3	22.1	1.7	22.8	24.9	18.9	14.0	52.1	2.0	15.37	23.01	11.63	16.54	19.70	13.54	0.94	1.48	0.76	1.35	1.48	1.28	3.3	4.8	1.0	
Swamp	12.7	23.0	0.9	31.6	44.9	16.6	37.7	70.9	2.6	12.82	13.62	12.29	17.16	18.29	16.58	0.75	0.81	0.67	1.28	1.32	1.23	4.5	4.7	4.2	

^aHigh, intermediate, and low refers to the hydrologic regime state during sampling (see section 2.1).

followed by acidification (pH = 1 with 12 N H₂SO₄) and extraction 3 times with ethyl acetate, passed through Na₂SO₄ drying columns, and taken to dryness under a gentle stream of ultrapure nitrogen. After redissolution in pyridine, lignin phenols were silylated (BSTFA) and quantified using gas chromatography mass spectrometry (GC-MS) (Agilent 6890 gas chromatograph equipped with an Agilent 5973 mass selective detector and a DB5-MS capillary column; 30 m, 0.25 mm inner diameter, Agilent) using cinnamic acid as an internal standard and a five-point calibration scheme. Eight lignin phenols were quantified for all samples, including three vanillyl phenols (vanillin, acetovanillone, and vanillic acid), three syringyl phenols (syringaldehyde, acetosyringone, and syringic acid), and two cinnamyl phenols (p-coumaric acid and ferulic acid). One blank was run for every 10-sample oxidations, and all samples were blank corrected. Blank concentrations of lignin phenols were low (30–40 ng) and consequently never exceeded 5% of the total lignin phenols in a sample. Lignin phenol concentrations are reported as the sum of the cinnamyl, syringyl, and vanillyl phenols (Σ_8). Additionally, the carbon-normalized sum of the lignin phenols (Λ_8) was also calculated.

2.7. DIC, pCO₂, and Gas Flux Calculations

DIC was measured using an autoanalyzer (AS-C3, Apollo SciTech) that purges CO₂ gas from an acidified water sample with a nitrogen carrier gas. The instrument was calibrated using certified reference materials (CRMs) from Dr. Andrew Dickson (Scripps Institution of Oceanography, University of California, San Diego) and has a precision and accuracy of approximately ±2 μmol L⁻¹. A modified Gran titration procedure [Wang and Cai, 2004] was used to determine the TA of the samples potentiometrically using an automated titrator (AS-ALK2, Apollo SciTech). The CRMs were also used to calibrate the TA titrator. TA measurements had a precision and accuracy of ±2 μmol L⁻¹.

The partial pressure of carbon dioxide (pCO₂) was calculated using measured DIC and pH values and the CO₂ program by Pierrot *et al.* [2006]. Areal CO₂ flux estimates were calculated using a simple gas transfer model, $F = k\alpha\Delta pCO_2$, where k is the gas transfer in freshwater, α the solubility of CO₂ [Weiss, 1974],

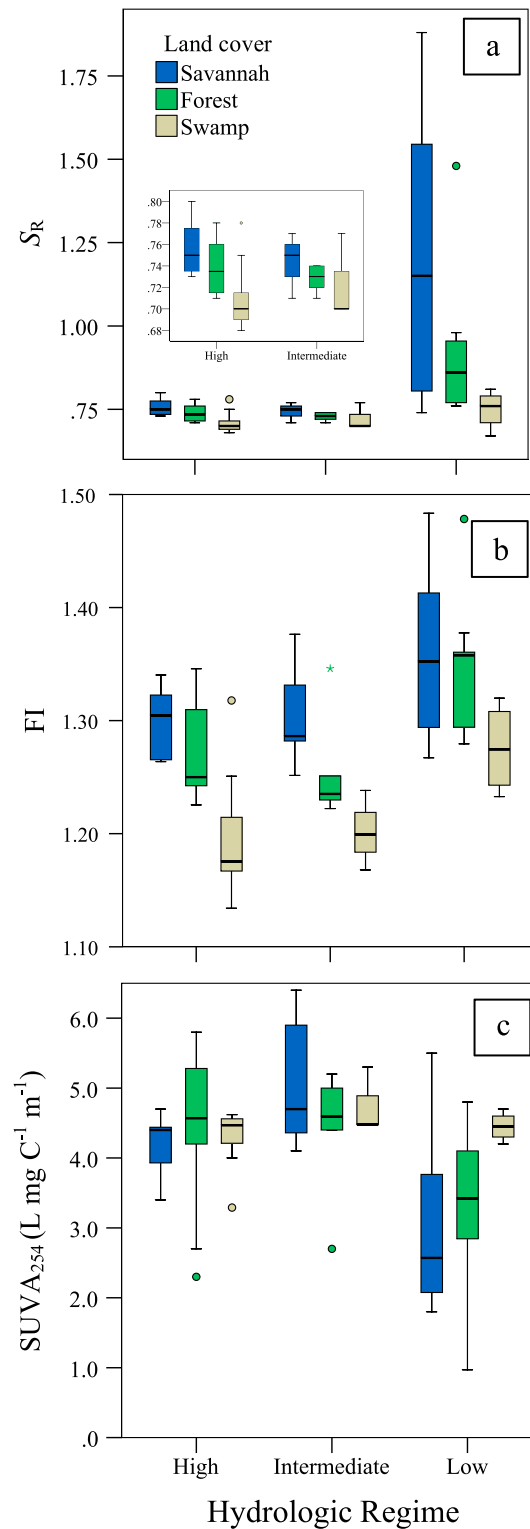


Figure 3. Boxplots of (a) S_R , (b) FI , and (c) $SUVA_{254}$ during high, intermediate, and low hydrologic conditions within each of the three land cover types (savannah, forest, and swamp). The black line within each box represents the mean, the height of each box denotes the 25th and 75th percentiles, and the error bars denote the 10th and 90th percentiles.

and ΔpCO_2 the pCO_2 gradient between water and air. The global atmospheric mean pCO_2 (390 μatm in 2010) was used for the flux calculations. Values for k were taken from a global synthesis of gas exchange velocities for tropical streams (< 100 m; $k_{600} = 17.2 \text{ cm h}^{-1}$) and rivers (> 100 m; $k_{600} = 12.3 \text{ cm h}^{-1}$), as well as wetlands ($k_{600} = 2.4 \text{ cm h}^{-1}$), and calculated for in situ temperature [Aufdenkampe *et al.*, 2011]. Recent measurements of k in other tropical rivers such as the Amazon and East Asian Rivers closely support these average stream ($k_{600} = 23.3 \pm 17.3 \text{ cm h}^{-1}$) and river values ($k_{600} = 14.7 \pm 8.6 \text{ cm h}^{-1}$) [Alin *et al.*, 2011].

2.8. Statistics

Normality was assessed using histograms and Shapiro-Wilk tests. Nonnormal data were log-transformed to allow the use of parametric statistics before analysis. Two-way analysis of variance was used to identify the main effects of land cover type and hydrologic regime and to assess for potential interactions between them (F_x , where x is degrees of freedom). Interactions relate to combined effects of land cover and hydrology and examine if there are significant differences in how different land cover types respond to changes in hydrologic regime. Posthoc tests were conducted using independent pairwise comparisons of significant effects. Pearson's correlation coefficients (R^2) were used to assess relationships between variable pairs. All statistical tests assumed a significance level of < 0.05 and were conducted using the SPSS 20 (IBM) software program.

3. Results

3.1. Seasonal and Spatial Patterns in DOC, a_{350} , and C:N

DOC concentration ranged from 0.9 to 81.2 $mg \text{ C L}^{-1}$ across all of the sites and sampling periods (Figure 2a and Table 1). DOC concentration was closely associated with hydrologic regime, with highest observed mean concentrations in streams during high flow conditions (21.1 $mg \text{ C L}^{-1}$; $n = 39$) and lowest at periods of reduced flow (6.8 $mg \text{ C L}^{-1}$; $n = 21$). DOC concentrations were consistently highest in waters from swamp-dominated catchments, intermediate in forest, and lowest in savannah regions (Figure 2a).

Sixteen percent of the variability in DOC concentrations was explained by hydrologic state alone ($F_2 = 7.3$, $p < 0.01$), whereas land cover

Table 2. Lignin Phenol Concentration (Σ_8), Carbon-Normalized Yield (Λ_8), Cinnamyl/Vanillyl Phenol Ratios, Syringyl/Vanillyl Phenol Ratios, Vanillic Acid/Vanillin Ratios, and Syringyl/Vanillyl Phenol Ratios^a

	Σ_8 ($\mu\text{g L}^{-1}$)			Λ_8 (mg (100 mg OC) ⁻¹)			C/V			S/V			(Ad/Al) _v			(Ad/Al) _s		
	Mean	Max	Min	Mean	Max	Min	Mean	Max	Min	Mean	Max	Min	Mean	Max	Min	Mean	Max	Min
High																		
Savannah	50.1	87.1	11.1	0.82	1.13	0.50	0.14	0.17	0.09	0.76	0.85	0.70	1.69	1.88	1.34	0.96	1.03	0.89
Forest	67.4	118.6	6.5	0.69	1.02	0.33	0.16	0.27	0.08	0.76	0.90	0.56	1.53	1.81	1.32	0.97	1.14	0.83
Swamp	139.4	184.2	16.9	0.43	0.96	0.25	0.16	0.18	0.12	0.79	0.85	0.73	1.43	1.47	1.31	0.97	1.13	0.81
Intermediate																		
Savannah	52.6	132.0	13.9	0.80	1.18	0.62	0.19	0.33	0.11	0.88	1.07	0.67	1.61	2.06	1.24	0.99	1.19	0.78
Forest	45.6	45.8	45.4	0.64	0.65	0.62	0.23	0.25	0.20	0.89	0.93	0.85	1.54	1.55	1.52	0.96	0.98	0.94
Swamp	-	-	-	-	-	-	-	-	-	-	-	-	-	-	-	-	-	-
Low																		
Savannah ^b	20.1	20.1	20.1	0.77	0.77	0.77	0.17	0.17	0.17	0.94	0.94	0.94	1.97	1.97	1.97	1.25	1.25	1.25
Forest	-	-	-	-	-	-	-	-	-	-	-	-	-	-	-	-	-	-
Swamp	71.7	163.9	5.8	0.83	1.74	0.26	0.24	0.41	0.13	0.87	1.03	0.64	1.61	1.96	1.39	1.07	1.15	0.93

^aHigh, intermediate, and low refers to the hydrologic regime state during sampling (see section 2.1).

^bOnly one sample was taken during this period.

properties explained 39% of the overall variance ($F_2 = 23.9$, $p < 0.001$). Differences in DOC concentrations with hydrologic state were also significantly dependent upon land cover type ($F_4 = 2.8$, $p < 0.05$). Swamp regions exported significantly higher proportions of DOC during high and intermediate flow conditions relative to low flow periods ($F_2 = 9.8$, $p < 0.01$), whereas land cover and hydrologic regime in forest and savannah regions independently controlled DOC concentrations.

CDOM absorbance coefficients (a_{350}) similarly varied in line with hydrologic regime over the study period (Figure 2b). Mean a_{350} values decreased from 62.1 m^{-1} ($n = 35$) during high flow conditions to 17.2 m^{-1} ($n = 19$) during dry periods, in conjunction with reductions in flow ($F_2 = 7.7$, $p < 0.01$). CDOM a_{350} values also varied significantly with land cover type ($F_2 = 21.7$, $p < 0.001$) (Table 1 and Figure 2b). C:N ratios ranged from 16.6 to 57.6 (mean = 33.3, $n = 58$), demonstrating higher ratios during high flow periods relative to intermediate and low hydrologic regime periods ($F_2 = 13.0$, $p < 0.001$). C:N ratios were significantly highest in swamp catchment waters relative to other land cover types ($F_2 = 7.8$, $p < 0.01$, Table 1).

3.2. Seasonal and Spatial Patterns in CDOM Optical Composition

S_R and $S_{275-295}$ values ranged between 0.67 and 1.88 (mean = 0.82; $n = 73$), and 10.19 to $30.62 \times 10^3 \text{ nm}^{-1}$ (mean = $13.56 \times 10^3 \text{ nm}^{-1}$; $n = 73$), respectively, over the duration of the study. Both S_R and $S_{275-295}$ significantly differed with hydrologic regime ($F_2 = 7.8$, 9.3, $p < 0.001$, respectively), displaying marked increases during periods of low flow (Table 1 and Figure 3a). FI values were significantly higher during low flow periods ($F_2 = 15.9$, $p < 0.001$; Figure 3b). No discernible patterns with hydrology were observed in the $S_{350-400}$ values (Table 1). DOM quality as inferred from S_R , $S_{350-400}$, and FI also varied across waters originating from different land cover types ($F_2 = 4.8$, 3.4, and 13.1, respectively, $p < 0.05$; Figures 3a and 3b). Effects of land cover and hydrologic regime on DOM composition were independent from one another in all but S_R values, which displayed significantly higher values in savannah and forest catchments during low flow periods ($F_4 = 2.5$, $p < 0.05$; Figure 3a). The spectral slope $S_{350-400}$ followed an opposing pattern to S_R , with highest values in swamp influenced catchments ($F_2 = 3.4$, $p < 0.05$). $SUVA_{254}$ values ranged widely from 1.0 to $5.9 \text{ L mg C}^{-1} \text{ m}^{-1}$ (mean = $4.2 \text{ L mg C}^{-1} \text{ m}^{-1}$; $n = 69$) over the study period and significantly differed with hydrologic regime ($F_2 = 6.9$, $p < 0.01$; Figure 3c). $SUVA_{254}$ values displayed no significant trends with land cover type during high and intermediate hydrologic regime states but were distinguishable during low water periods (Table 1 and Figure 3c).

3.3. Seasonal and Spatial Patterns in Lignin

Σ_8 and Λ_8 ranged over the course of the study from 5.8 to $184.2 \mu\text{g L}^{-1}$ (mean = $72.8 \mu\text{g L}^{-1}$; $n = 36$), and 0.25 to $1.74 \text{ (mg (100 mg OC)}^{-1})$ (mean = $0.70 \text{ (mg (100 mg OC)}^{-1})$; $n = 36$), respectively (Table 2). C/V and S/V phenol ratios ranged from 0.08 to 0.41 (mean = 0.17; $n = 36$) and 0.56 to 1.07 (mean = 0.81; $n = 36$), respectively (Figure 4a). Land cover properties significantly impacted Σ_8 values, swamp forests delivering

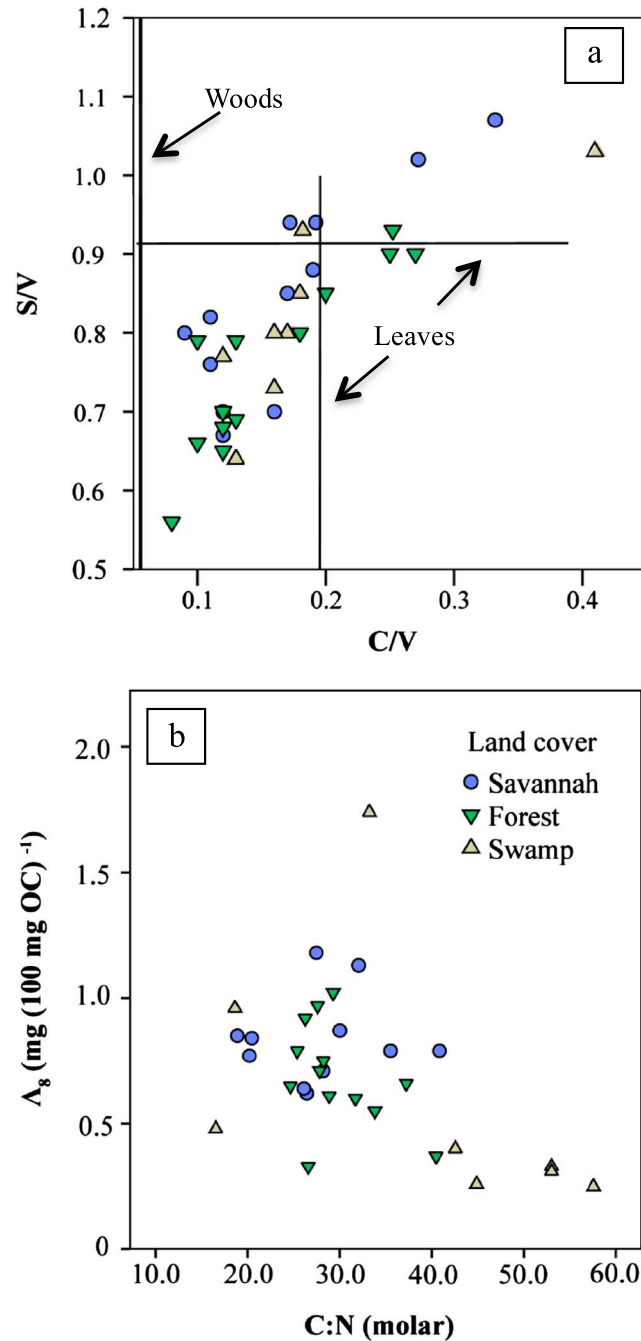


Figure 4. (a) Lignin compositional parameters, C/V versus S/V for samples collected from each land cover type (see legend). Lines represent the median and range of values for dicotyledonous leaves and woody tissues [Hedges *et al.*, 1986]. (b) C:N (molar) versus carbon-normalized lignin (Λ_8).

higher overall lignin concentrations than savannah, or forest catchments ($F_2 = 3.5, p < 0.05$). The distribution of S/V phenols varied significantly across the hydrograph ($F_2 = 3.4, p < 0.05$) with mean values increasing from 0.77 during high flow periods to 0.89 at low flow (Table 2). Other than S/V, no other lignin parameters demonstrated significant differences with hydrologic regime (Table 2).

3.4. Variation in pH, DIC, and Total Alkalinity

The pH values ranged between 3.56 and 7.90 across study sites and hydrologic regimes ($n = 91$; Table 3). Mean pH decreased with increases in the hydrologic regime ($F_2 = 6.5, p < 0.001$), in good agreement with observations from the Congo River main stem [Wang *et al.*, 2013]. Land cover type also influenced freshwater pH ($F_2 = 18.2, p < 0.001$), with swamps exporting more acidic waters (mean = 4.42; $n = 27$) compared to nearer neutral conditions in waters from forest-dominated catchments (mean = 6.00; $n = 39$; Table 3).

DIC values ranged from 91.4 to 531.6 $\mu\text{mol L}^{-1}$ (mean = 301.0 $\mu\text{mol L}^{-1}$; $n = 28$; Table 3) and were significantly higher in swamp-influenced streams (400.2 $\mu\text{mol L}^{-1}$; $n = 9$) than in savannah (233.1 $\mu\text{mol L}^{-1}$; $n = 7$) or forest streams (265.5 $\mu\text{mol L}^{-1}$; $n = 12$) ($F_2 = 3.7, p < 0.05$). Mean DIC concentrations were significantly higher under low flow conditions (mean = 466.7 $\mu\text{mol L}^{-1}$; $n = 2$), relative to high flow periods (mean = 233.1 $\mu\text{mol L}^{-1}$; $n = 19$) ($F_2 = 4.4, p < 0.5$). No combined influence of land cover on hydrologic regime was observed in either pH or DIC. TA varied between 0 and 241.7 $\mu\text{mol L}^{-1}$ ($n = 28$) and was often very low or below the detection limit ($< 10 \mu\text{mol L}^{-1}$), which is consistent with generally low pH conditions (Table 3).

3.5. The $p\text{CO}_2$ Concentration and CO_2 Efflux Rates

In situ $p\text{CO}_2$ ranged between 2600 and 15,802 μatm (Table 3). Mean $p\text{CO}_2$ values differed significantly with land cover type ($F_2 = 8.0, p < 0.01$) and hydrologic regime ($F_2 = 4.4, p < 0.05$; Figure 5). Highest $p\text{CO}_2$ values were consistently calculated in waters from swamp catchments (mean = 12,858 μatm , $n = 6$), and

Table 3. Mean, Median, Maximum, and Minimum Values for pH, Dissolved Inorganic Carbon, Total Alkalinity, and $p\text{CO}_2$ for Streams and Rivers Draining Each Land Cover Type Studied

	pH				DIC ($\mu\text{mol L}^{-1}$)				TA ($\mu\text{mol L}^{-1}$)				$p\text{CO}_2$ (μatm)			
	Mean	Median	Max	Min	Mean	Median	Max	Min	Mean	Median	Max	Min	Mean	Median	Max	Min
Savannah	5.48	5.10	7.90	3.75	233.1	221.0	401.7	91.9	37.0	0.0	181.1	0.0	5,851	5,296	11,922	2,739
Forest	6.00	6.28	7.68	4.15	265.5	286.7	380.9	91.4	48.0	13.1	241.7	0.0	6,631	6,866	10,740	2,600
Swamp	4.42	4.43	5.71	3.56	400.2	402.0	531.6	224.0	0.0	0.0	0.0	0.0	12,858	12,474	15,802	10,598

lowest in savannah catchment waters (mean = 5851 μatm , $n = 7$; Figure 5). Forested catchments displayed intermediate $p\text{CO}_2$ values approximately half of those reported in swamp regions (mean = 6631 μatm , $n = 12$; Table 3). Mean in-situ $p\text{CO}_2$ was significantly higher during low discharge periods, as compared to intermediate and high flow conditions (Table 4). This increase was due to increased $p\text{CO}_2$ in savannah regions during low flow periods, whereas swamp forest waters varied little with hydrologic regime ($F_4 = 5.2$, $p < 0.05$).

Using a widely applied gas evasion model (see section 2.7) and published tropical inland water gas exchange velocity values corrected for in situ water temperatures [Aufdenkampe *et al.*, 2011], we estimated mean areal CO_2 evasion rates. Estimated mean rates ranged between 312 and 1429 $\text{mmol CO}_2 \text{ m}^{-2} \text{ d}^{-1}$ or 3.7 and 17.1 $\text{g C m}^{-2} \text{ d}^{-1}$ across all study sites (Table 4). Mean evasion rates were similar in streams and rivers from each land cover type, swamp waters demonstrating the lowest evasion rates and tropical forest waters the highest (Table 4). This trend was opposite to that of $p\text{CO}_2$ demonstrating the important role of gas transfer velocities (k) in flux calculations. The use of fixed exchange velocities (k) here will result in error, but allow for general patterns across land cover types, and streams and rivers to be examined assuming global trends in k translate to the Congo Basin. Direct measurements of k in flowing waters globally range from 3 to 30 cm h^{-1} [Aufdenkampe *et al.*, 2011, supplemental data]. Assuming lower k values and correcting for temperature, stream and river waters in savannah and forest basins would evade between 4.1 and 5.7 times lower quantities of CO_2 than we estimate (Table 4), but swamp water fluxes stay similar due to low initial k values.

Assuming higher k values, savannah and forest waters would be expected to evade 1.7 to 2.4 greater amounts of CO_2 , but swamp water outgassing estimates would increase by 12.5 times (up to 4627 $\text{mmol CO}_2 \text{ m}^{-2} \text{ d}^{-1}$ or 55.5 $\text{g C m}^{-2} \text{ d}^{-1}$).

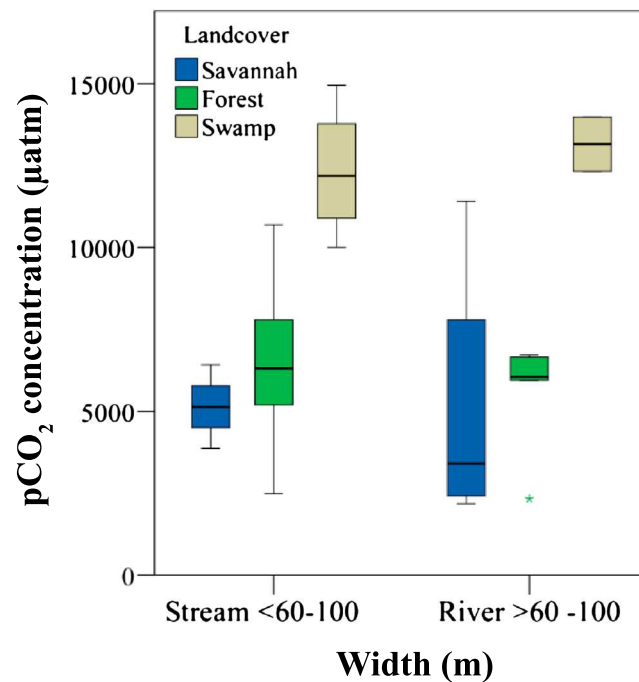


Figure 5. Boxplot of $p\text{CO}_2$ from streams and rivers separated by channel width (< 100 m or > 100 m) and land cover type. The black line within each box represents the mean, the height of each box denotes the 25th and 75th percentiles, and the error bars denote the 10th and 90th percentiles.

4. Discussion

4.1. Hydrologic and Land Cover Controls Upon Stream Carbon Export

The DOC concentration and DOM quality in streams and rivers across the Congo Basin can be significantly influenced by land cover type and hydrologic conditions. Broad-scale land cover properties, derived from satellite information, explained the greatest proportion of variance in freshwater DOC concentration (39%) and a_{350} (40%), more than twice that of hydrology (16% and 19%, respectively). This indicates that subbasin vegetation properties predominantly control overall C export patterns. Higher DOC concentrations in swamp and wetland

Table 4. Mean and Median $p\text{CO}_2$ Values Measured in Streams (< 100 m Wide) and Rivers (>100 m Width) From Each Land Cover Type Studied^a

Land Cover Type		n.	$p\text{CO}_2$ (μatm)			Areal Outgassing Rate	
			Mean	Median	k_{600} [#]	($\text{mmol CO}_2 \text{ m}^{-2} \text{ d}^{-1}$)	($\text{g C m}^{-2} \text{ d}^{-1}$)
Savannah	Rivers (>100 m wide)	2	6,303	5,275	12.3	$1,064 \pm 999$	12.8 ± 12.0
	Streams (< 100 m wide)	4	5,249	5,296	17.2	$1,282 \pm 497$	15.4 ± 6.0
Forest	Rivers (> 100 m wide)	7	6,620	7,141	12.3	862 ± 235	10.3 ± 2.8
	Streams (< 100 m wide)	5	6,639	6,333	17.2	$1,429 \pm 695$	17.1 ± 8.3
Swamp	Rivers (> 100 m wide)	2	13,165	13,165	2.4	370 ± 40	4.4 ± 0.5
	Streams (< 100 m wide)	5	12,704	12,208	2.4	312 ± 126	3.7 ± 1.5

^aAreal daily outgassing rates were calculated using published gas transfer velocities[#] for tropical streams and rivers ([#] k_{600}) [Aufdenkampe et al., 2011] adjusted for site temperature.

waters during intermediate to high flow conditions demonstrate that increased precipitation and runoff can act as a mechanism for releasing greater proportions of C in these regions. C:N ratios of waters were explained by both land cover properties (18%) and hydrologic regime (24%) independently, suggesting that the C:N in streams in subbasins is controlled by both regional vegetation type and precipitation patterns.

Dissolved lignin phenols are unambiguous biomarkers of vascular plant material, thus their presence and composition provide information pertaining to C source. Despite swamp environments exporting significantly higher Σ_8 concentrations relative to other vegetation types, lack of distinct differences in carbon-normalized lignin phenol yields (Λ_8) suggest that the proportion of vascular plant material contributing to the overall DOC pool remains relatively constant across vegetation types and hydrologic flow conditions. Significant positive linear relationships were observed between DOC and Σ_8 across all sites ($p < 0.05$), with the slope of the relationship varying among land cover types. Savannah environments (slope $y = 0.5$, $R^2 = 0.90$) exported higher Σ_8 concentrations per unit C (Λ_8) relative to forest ($y = 20.7$, $R^2 = 0.62$) and swamp environments ($y = 42.9$, $R^2 = 0.67$). Savannah waters therefore contained higher proportions of vascular plant material relative to forest and swamp waters. The lack of a significant relationship between Λ_8 and DOC across any of the sites indicates that as freshwater DOC concentration changed, the proportion of vascular plant material also shifted, indicating a change in DOC source over the season.

DIC concentrations were significantly higher during drier months, and lowest during high discharge periods. DIC concentrations were also independently controlled by vegetation cover, with swamp regions exporting waters containing almost twice the mean DIC concentration than forest and savannah waters (Table 3). This apparent inverse relationship between DIC concentration and discharge suggests a seasonal shift in dominant flow paths where highest contributions of deeper soil flow waters with elevated DIC concentrations occur during lower flow conditions. Rapid overland flow paths, associated with rainy season high-discharge conditions, can contribute an order of magnitude higher DOC fluxes than delivered by deeper groundwater flow in Amazonian headwater catchments [Johnson et al., 2006]. Taken together, our findings suggest a tightly coupled link between the hydrologic and carbon cycles, with organic C supply primarily controlled by overland and surface flow paths, and inorganic C by deeper groundwater pathways (Tables 1 and 3). Land cover properties, in turn, strongly influence the availability of organic C to be exported to stream and rivers and can affect how subbasins regulate C release after precipitation events.

Tropical watersheds globally are being transformed by expanding agricultural and logging activities, as well as global and regional climate change effects [Davidson et al., 2012; Laporte et al., 2007]. Future predicted changes for these regions include anthropogenic impacts such as construction of dams and altered precipitation patterns, with resultant impacts upon river discharge patterns, and shifts in vegetation from rainforest to savannah ecosystems [Aerts et al., 2006; Koenig, 2008; Spencer et al., 2014]. Our findings suggest that increased subbasin coverage of savannah vegetation would result in a reduction in the overall fluvial DOC concentration but a relative increase in the proportion of the DOC pool supplied from vascular plants.

4.2. Organic Matter Composition

An overall reduction in the apparent aromaticity and molecular weight of the DOM pool was observed during low hydrologic conditions relative to intermediate and high runoff periods, as inferred from $S_{275-295}$, S_R , Fl ,

and SUVA₂₅₄ indices (Figures 3a–3c). Savannah and forest catchments in particular, displayed a marked reduction in the apparent aromaticity and molecular weight of DOM exported during low flow conditions (elevated S_R values). Swamp influenced subbasins displayed little or even opposing trends to other vegetation types, demonstrating that they persistently export greater proportions of apparent aromatic and higher molecular weight DOM throughout the year (Figures 3a–3c). These findings compare well with previous observations that wetlands and swamps are associated with more aromatic, higher molecular weight organics [Mladenov *et al.*, 2007; Pinney *et al.*, 2000] and that these environments can moderate carbon composition and export as previously reported in the Amazon [Johnson *et al.*, 2006].

Similar temporal shifts in DOM composition have been reported in a range of temperate and tropical watersheds [Sanderman *et al.*, 2009; Spencer *et al.*, 2010a; Yamashita *et al.*, 2010]. These studies attribute the observed changes in DOM composition to shifting source material from predominantly surface, younger organic-rich horizons during high flow periods, to older soil-derived deeper organic matter during drier conditions.

As DOM reactivity (biological and photochemical) is strongly related to its chemical composition, shifting freshwater DOM quality will influence the efficiency and extent of C processing within inland waters. Our results demonstrate that with predicted increases to dry-season duration, as well as changing vegetation patterns [Aerts *et al.*, 2006; Koenig, 2008; Spencer *et al.*, 2014], we can expect an associated reduction in the overall molecular weight and aromaticity of the exported DOM pool influencing the biogeochemistry of coastal environments and the role of inland waters as processors of terrigenous C.

4.3. Organic Matter Sources and Processing

In order to examine if DOC turnover could explain the C concentration patterns we observed across subbasins, we conducted a series of linear regressions comparing catchment size—a simple proxy of residence time [e.g., Worrall *et al.*, 2012]—with DOC concentration. We included both explanatory and response variables untransformed and log-transformed. Across all sample dates and sites, a weak yet significant negative relationship between log-transformed area and log-transformed DOC concentration was observed ($R^2 = 0.14$, $p < 0.01$, $n = 85$; Figure 6a). These relationships persisted during high ($R^2 = 0.11$, $p < 0.05$, $n = 39$) and low flow periods ($R^2 = 0.30$, $p < 0.01$, $n = 21$), but not during intermediate discharge conditions ($p = 0.12$, $n = 25$). Separating by land cover, relationships were only present in forest and swamp environments ($R^2 = 0.15$, 0.20 , $p < 0.05$, $n = 39$, 22 , respectively) with savannah subcatchments spanning a relatively small gradient in basin sizes. These relationships indicate that DOC turnover via physical or biological processes can be observed in bulk DOC concentrations throughout the basin, particularly during low flow periods when longer residence times may promote greater in situ production and respiration.

Lignin phenol ratios are used extensively to provide detailed source and diagenetic processing information [Hedges and Mann, 1979; Hernes and Benner, 2003]. The discrimination of gymnosperm and angiosperm sources, for example, can be examined using the ratio of syringyl (S) to vanillyl (V) phenols, or the contribution of woody to nonwoody tissues estimated using ratios of cinnamyl (C) to V phenols [Hedges and Mann, 1979]. Plotting sample S/V versus C/V shows that our stream and river DOM originates from a mixture of nonwoody tissues predominantly of angiosperm origin (Figure 4a) [Hedges and Mann, 1979; Spencer *et al.*, 2010a]. Mean S/V ratios decreased modestly but significantly with increasing discharge (Table 2), indicating shifting source inputs or alterations in the extent of processing or leaching of source materials over the season. This contrasts with a small tributary of the Congo River that exhibited no changes in S/V in any season, despite significant differences in discharge [Spencer *et al.*, 2010a], which is likely related to difference in soil structure. C/V and S/V ratios displayed significant linear increases with increasing catchment area, particularly in forest and swamp-dominated environments (Figures 6b and 6c). S/V ratios are sensitive to DOM photolysis with decreases in S/V interpreted as evidence of photooxidation [Benner and Opsahl, 2001; Hernes and Benner, 2003]. S/V ratios appear to be largely unaffected by short-term microbial incubations and flocculation processes in freshwaters [Hernes and Benner, 2003]. The increasing S/V and C/V ratios we observed during transport are therefore likely caused by changing physical conditions such as leaching and sorption processes [Hernes *et al.*, 2013, 2007].

Organic matter sources have further been discriminated by combining C:N measurements with Λ_8 [e.g., Gøñi *et al.*, 1998, 2006; Spencer *et al.*, 2012a]. DOM from swamp catchments generally contained lower Λ_8 values

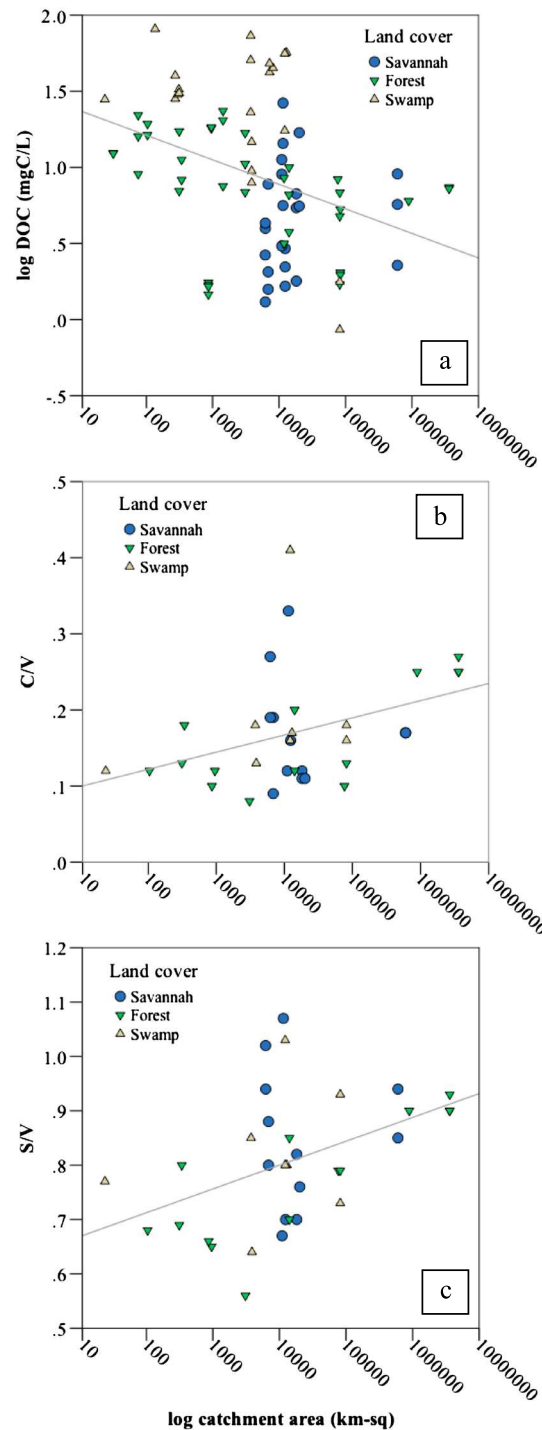


Figure 6. (a) Log DOC concentration against log catchment area. Line represents the linear regression ($R^2 = 0.14$, $p < 0.05$) across all sites. Lignin phenol ratios (b) C/N and, (c) S/V across log catchment area. Line represents the linear regression across all sites ($R^2 = 0.15$, 0.20 , $p < 0.05$, respectively).

and higher C:N ratios than other catchment types (Tables 1 and 2), consistent with lower vascular plant inputs from tree and woody vegetation combined with high-overall carbon export patterns (Figure 4b). Swamp waters may therefore contain enriched quantities of vascular plant-derived polysaccharides (lower Λ_8) yet contain sufficient tannins and other optically active moieties to result in similar CDOM per unit DOC ($SUVA_{254}$) values under most hydrographic conditions (Figure 3c) [Hernes et al., 2001; Hernes and Hedges, 2004]. Generally higher Λ_8 values from tropical forest and savannah catchments alongside more moderate C:N ratios suggest higher vascular plant vegetation export from C3-dominated regions in these catchments (Figure 4b).

Ratios of $(Ad/Al)_v$ and $(Ad/Al)_s$ are frequently used as an indicator of the degradative state of DOM [Hernes and Benner, 2003; Hernes et al., 2008; Spencer et al., 2009]. Although direct comparisons between $(Ad/Al)_v$ values and land cover types should be undertaken with care, due to potential lignin fractionation effects that can occur in DOM by leaching and sorption processes [Hernes et al., 2007], trends at individual sites measured repeatedly across the year are likely informative. Increases in both $(Ad/Al)_v$ and $(Ad/Al)_s$ values were observed at all six sites with decreasing discharge, except for one savannah site which displayed decreases in $(Ad/Al)_v$ values. High (Ad/Al) ratios indicate greater oxidation, and (Ad/Al) ratios can increase with greater microbial degradation [Hernes and Benner, 2003; Pellerin et al., 2010]. Combined, our results indicate that an increased proportion of deep soil flow water is present in streams and rivers during drier conditions, and that increased soil residence time and changing hydrologic flow paths enable more extensive prior processing, sorption, and partitioning of the DOM pool before export [Spencer et al., 2010a; Striegl et al., 2005]. These processes result in a more degraded DOM signature (e.g., reduced aromaticity, molecular weight, and higher FI) during these periods.

4.4. CO₂ Evasion

All streams and rivers measured throughout the Congo Basin were supersaturated in pCO_2 indicating that they were net sources of CO₂ to

the atmosphere (Tables 3 and 4). Surface water pCO_2 throughout the Congo Basin, excluding swamp waters were comparable (2,600–11,922 μatm) but ranged more than those previously reported from the Amazon ($4,350 \pm 1,900 \mu\text{atm}$) [Richey et al., 2002] and Congo River main stems (2,018–6,853 μatm) [Wang et al., 2013],

and other African rivers such as the Nyong Basin in Cameroon ($7,245 \pm 3,046 \mu\text{atm}$) [Brunet et al., 2009]. Our forest and savannah median $p\text{CO}_2$ values ($5275\text{--}7141 \mu\text{atm}$) were higher than those reported in a global synthesis of tropical inland water gas measurements that estimated $4300 \mu\text{atm}$ and $3600 \mu\text{atm}$ for tropical streams ($<100 \text{ m}$) and rivers ($>100 \text{ m}$), respectively, [Aufdenkampe et al., 2011] (Table 4). Our findings contrast with those from the Oubangui River, a major tributary of the Congo River, where mean $p\text{CO}_2$ values were notably lower (1678 ± 1092) than the global synthesis estimates [Bouillon et al., 2012]. The predominant savannah vegetation cover of the Oubangui catchment, and the relatively low $p\text{CO}_2$ values of savannah-dominated catchments in this study provide strong rationale as to the lower values in the Oubangui (Table 4).

Our study showed that swamp forest waters within the Congo Basin contained extremely high $p\text{CO}_2$ concentrations ($10,598\text{--}15,802 \mu\text{atm}$) with median values in streams ($12,208 \mu\text{atm}$) and rivers ($13,165 \mu\text{atm}$) far greater than those reported for global wetland regions ($2,900 \mu\text{atm}$) [Aufdenkampe et al., 2011]. Aquatic CO_2 supersaturation throughout Amazonian Rivers represents a significant component of regional carbon budgets [Mayorga et al., 2005; Richey et al., 2002]. In this study, mean areal CO_2 outgassing rates were estimated to range between 312 and $1429 \text{ mmol m}^{-2} \text{ d}^{-1}$ in streams ($<100 \text{ m}$ width) and from 370 to $1064 \text{ mmol m}^{-2} \text{ d}^{-1}$ in rivers ($>100 \text{ m}$ width), for the periods of our study (Table 4). These fluxes are comparable but higher than recent estimates of CO_2 flux from an annual study of the Congo River main stem at Brazzaville of between 133 and $506 \text{ mmol CO}_2 \text{ m}^{-2} \text{ d}^{-1}$ [Wang et al., 2013]. Previous measurements of $\delta^{13}\text{C}$ of respired CO_2 collected from tropical streams and rivers has suggested that no single organic matter source consistently fuels CO_2 evasion and that C source varies spatially and temporally [Mayorga et al., 2005]. Groundwater inputs of CO_2 can act as a large source of terrestrially respired CO_2 particularly in tropical headwaters [Johnson et al., 2008; Richey et al., 2009], which could account for the high $p\text{CO}_2$ values observed here. The similarity and persistence of $p\text{CO}_2$ observed in this study throughout the river network from smaller streams ($<100 \text{ m}$) and larger rivers ($>100 \text{ m}$) however suggests a downstream source of CO_2 that is in close equilibrium with outgassing rates. The production of CO_2 from in situ respiration of autochthonous- and allochthonous-derived organic matter sources has previously been reported with terrigenous DOM fueling a significant proportion of CO_2 evasion [Mayorga et al., 2005; Richey et al., 1990; Ward et al., 2013]. Across our sites, in situ $p\text{CO}_2$ was positively correlated with DOC concentration ($R^2 = 0.54$, $p < 0.01$, $n = 24$) and Σ_8 ($R^2 = 0.33$, $p < 0.01$, $n = 16$). Water $p\text{CO}_2$ was also strongly inversely correlated with percent oxygen saturation ($R^2 = 0.92$, $p < 0.001$, $n = 24$) and Λ_8 ($R^2 = 0.42$, $p < 0.01$, $n = 16$). Hence, it seems likely that a proportion of CO_2 and subsequent greenhouse gas efflux, especially in large streams and rivers away from headwater influences, originated from allochthonous DOC inputs [Hamilton et al., 1995; Mayorga et al., 2005; Ward et al., 2013]. The relatively low overall evasion rates we report from swamp subbasins, despite high water-air $p\text{CO}_2$ gradients, were caused by very low published estimates for k ($2.4 \text{ cm h}^{-1}/20^\circ\text{C}$) [Aufdenkampe et al., 2011]. Our results underpin that tropical inland waters may play a significant role in the processing of terrigenous organic matter and have the potential to be important pathways that must be considered in constructing regional carbon budgets. The vast range in $p\text{CO}_2$ measured across our sites demonstrates the critical importance of sampling over adequate spatial, as well as temporal scales, in order to correctly upscale regional or basin-scale estimates for CO_2 fluxes. Accurately parameterizing air-water flux rates will be critical for determining the relative importance of these regions on greenhouse gas budgets under natural and anthropogenically influenced conditions.

4.5. Basin-Scale Optical Proxies for DOM

Optical parameters provide high-resolution, cost-effective proxies for DOM concentration and composition, and therefore potential insights into DOM dynamics and reactivity [Fellman et al., 2010; Mann et al., 2012; Spencer et al., 2012b, 2013, 2008]. DOC concentrations and a_{350} values were significantly correlated over the entire study period and across all sample sites, ($R^2 = 0.98$, $df = 72$, $p < 0.001$) demonstrating the excellent potential for deriving DOC estimates from inexpensive optical properties, that can be measured at high temporal resolution using in situ instrumentation [Pellerin et al., 2011]. These strong linear relationships persisted and displayed identical slopes when the data were split into savannah, forest, and swamp subsets ($R^2 = 0.93$, 0.87 , 0.99 , $p < 0.001$, respectively) demonstrating that relationships were robust across the Congo Basin. Watershed-scale linear relationships between a_{350} and Σ_8 were significant but less strong ($R^2 = 0.65$, $df = 30$, $p < 0.001$). Relationships between a_{350} and Σ_8 were strongest in savannah-dominated catchments

($R^2 = 0.82$, $p < 0.001$) but, although still significant, were weaker in forest and swamp regions ($R^2 = 0.55$, 0.66 , $p < 0.05$, respectively). These regions must therefore contain significant and variable sources of other aromatics/phenolics, independent of lignin as discussed above. Our study demonstrates that optical measurements can provide valuable robust estimates of DOC concentrations and DOM properties that may prove useful for future studies aiming to examine carbon biogeochemistry in such a remote and challenging region to sample as the Congo Basin.

Acknowledgments

We would like to especially thank Paul Telfer and all of the members of the Congo Wildlife Conservation Society (WCS-Congo) for their fantastic logistical support and invaluable expert knowledge. We are particularly grateful to Jean-Pierre Tathy of the Groupe de Recherche en Sciences Exactes et Naturelles (GRSEN) for his continued help with our research and for aiding our close collaborations with our Congolese researchers. This work was supported by the National Science Foundation as part of the ETBC Collaborative Research: Controls on the Flux, Age, and Composition of Terrestrial Organic Carbon Exported by Rivers to the Ocean (0851101 and 0851015).

References

- Aerts, J. C. J. H., H. Renssen, P. J. Ward, H. de Moel, E. Odada, L. M. Bouwer, and H. Goosse (2006), Sensitivity of global river discharges under Holocene and future climate conditions, *Geophys. Res. Lett.*, *33*, L19401, doi:10.1029/2006GL027493.
- Aiken, G. R., H. Hsu-Kim, and J. N. Ryan (2011), Influence of dissolved organic matter on the environmental fate of metals, nanoparticles, and colloids, *Environ. Sci. Technol.*, *45*(8), 3196–3201, doi:10.1021/es103992s.
- Aitkenhead, J. A., and W. H. McDowell (2000), Soil C:N ratio as a predictor of annual riverine DOC flux at local and global scales, *Global Biogeochem. Cycles*, *14*(1), 127–138, doi:10.1029/1999GB900083.
- Alin, S. R., M. d. F. L. Rasera, C. I. Salimon, J. E. Richey, G. W. Holtgrieve, A. V. Krusche, and A. Snidvongs (2011), Physical controls on carbon dioxide transfer velocity and flux in low-gradient river systems and implications for regional carbon budgets, *J. Geophys. Res.*, *116*, G01009, doi:10.1029/2010JG001398.
- Aufdenkampe, A. K., E. Mayorga, P. A. Raymond, J. M. Melack, S. C. Doney, S. R. Alin, R. E. Aalto, and K. Yoo (2011), Riverine coupling of biogeochemical cycles between land, oceans, and atmosphere, *Front. Ecol. Environ.*, *9*(1), 53–60, doi:10.1890/100014.s01.
- Battin, T. J., S. Luysaert, L. A. Kaplan, A. K. Aufdenkampe, A. Richter, and L. J. Tranvik (2009), The boundless carbon cycle, *Nat. Geosci.*, *2*(9), 598–600, doi:10.1038/ngeo0618.
- Benner, R., and S. Opsahl (2001), Molecular indicators of the sources and transformations of dissolved organic matter in the Mississippi River Plume, *Org. Geochem.*, *32*, 597–607.
- Bouillon, S., A. Yambélé, R. G. M. Spencer, D. P. Gillikin, P. J. Hernes, J. Six, R. Merckx, and A. V. Borges (2012), Organic matter sources, fluxes and greenhouse gas exchange in the Oubangui River (Congo River basin), *Biogeochemistry*, *9*(6), 2045–2062, doi:10.1007/s10533-012-9204-2.
- Brunet, F., K. Dubois, J. Veizer, G. R. N. Ndong, J. R. N. Ngoupayou, J. L. Boeglin, and J. L. Probst (2009), Terrestrial and fluvial carbon fluxes in a tropical watershed: Nyong Basin, Cameroon, *Chem. Geol.*, *265*(3–4), 563–572, doi:10.1016/j.chemgeo.2009.05.020.
- Bwangoy, J.-R. B., M. C. Hansen, D. P. Roy, G. De Grandi, and C. O. Justice (2010), Wetland mapping in the Congo Basin using optical and radar remotely sensed data and derived topographical indices, *Remote Sens. Environ.*, *114*(1), 73–86, doi:10.1016/j.rse.2009.08.004.
- Cole, J. J., et al. (2007), Plumbing the global carbon cycle: Integrating inland waters into the terrestrial carbon budget, *Ecosystems*, *10*(1), 172–185, doi:10.1007/s10021-006-9013-8.
- Cory, R. M., and D. M. McKnight (2005), Fluorescence spectroscopy reveals ubiquitous presence of oxidized and reduced quinones in dissolved organic matter, *Environ. Sci. Technol.*, *39*(21), 8142–8149, doi:10.1021/es0506962.
- Coynel, A., P. Seyler, H. Etcheber, M. Meybeck, and D. Orange (2005), Spatial and seasonal dynamics of total suspended sediment and organic carbon species in the Congo River, *Global Biogeochem. Cycles*, *19*, GB4019, doi:10.1029/2004GB002335.
- Davidson, E. A., et al. (2012), The Amazon Basin in transition, *Nature*, *481*(7381), 321–328, doi:10.1038/nature10717.
- Del Vecchio, R., and N. V. Blough (2004), On the origin of the optical properties of humic substances, *Environ. Sci. Technol.*, *38*(14), 3885–3891, doi:10.1021/es049912h.
- Fellman, J. B., E. Hood, and R. G. M. Spencer (2010), Fluorescence spectroscopy opens new windows into dissolved organic matter dynamics in freshwater ecosystems: A review, *Limnol. Oceanogr.*, *55*(6), 2452–2462, doi:10.4319/lo.2010.55.6.2452.
- Goñi, M. A., K. C. Ruttenberg, and T. I. Eglinton (1998), A reassessment of the sources and importance of land-derived organic matter in surface sediments from the Gulf of Mexico, *Geochim. Cosmochim. Acta*, *62*(18), 3055–3075, doi:10.1016/S0016-7037(98)00217-8.
- Goñi, M. A., N. Monacci, R. Gisewhite, and A. Ogston (2006), Distribution and sources of particulate organic matter in the water column and sediments of the Fly River Delta, Gulf of Papua (Papua New Guinea), *Estuarine Coastal Shelf Sci.*, *69*(1–2), 225–245.
- Hamilton, S. K., S. J. Sippel, and J. M. Melack (1995), Oxygen depletion and carbon dioxide and methane production in waters of the Pantanal wetland of Brazil, *Biogeochemistry*, *30*(2), 115–141, doi:10.1007/BF00002727.
- Hedges, J. I., and J. R. Ertel (1982), Characterization of lignin by gas capillary chromatography of cupric oxide oxidation products, *Anal. Chem.*, *54*(2), 174–178, doi:10.1021/ac00239a007.
- Hedges, J. I., and D. C. Mann (1979), The characterization of plant tissues by their lignin oxidation products, *Geochim. Cosmochim. Acta*, *43*(11), 1803–1807. [online]
- Hedges, J. I., W. A. Clark, P. D. Quay, J. E. Richey, A. H. Devol, and U. d. M. Santos (1986), Compositions and fluxes of particulate organic material in the Amazon River, *Limnol. Oceanogr.*, *31*, 717–738.
- Helms, J. R., A. Stubbins, J. D. Ritchie, and E. C. Minor (2008), Absorption spectral slopes and slope ratios as indicators of molecular weight, source, and photobleaching of chromophoric dissolved organic matter, *Limnol. Oceanogr.*, *53*(3), 955–969.
- Hernes, P. J., and R. Benner (2003), Photochemical and microbial degradation of dissolved lignin phenols: Implications for the fate of terrigenous dissolved organic matter in marine environments, *J. Geophys. Res.*, *108*(C9), 3291, doi:10.1029/2002JC001421.
- Hernes, P. J., and J. I. Hedges (2004), Tannin signatures of barks, needles, leaves, cones, and wood at the molecular level, *Geochim. Cosmochim. Acta*, *68*(6), 1293–1307.
- Hernes, P. J., R. Benner, G. L. Cowie, M. A. Goñi, B. A. Bergamaschi, and J. I. Hedges (2001), Tannin diagenesis in mangrove leaves from a tropical estuary: A novel molecular approach, *Geochim. Cosmochim. Acta*, *65*(18), 3109–3122, doi:10.1016/S0016-7037(01)00641-X.
- Hernes, P. J., A. C. Robinson, and A. K. Aufdenkampe (2007), Fractionation of lignin during leaching and sorption and implications for organic matter “freshness,” *Geophys. Res. Lett.*, *34*, L17401, doi:10.1029/2007GL031017.
- Hernes, P. J., R. G. M. Spencer, R. Y. Dyda, B. A. Pellerin, P. A. M. Bachand, and B. A. Bergamaschi (2008), The role of hydrologic regimes on dissolved organic carbon composition in an agricultural watershed, *Geochim. Cosmochim. Acta*, *72*(21), 5266–5277, doi:10.1016/j.gca.2008.07.031.
- Hernes, P. J., B. A. Bergamaschi, R. S. Eckard, and R. G. M. Spencer (2009), Fluorescence-based proxies for lignin in dissolved organic matter, *J. Geophys. Res.*, *114*, G00F03, doi:10.1029/2009JG000938.
- Hernes, P. J., K. Kaiser, R. Y. Dyda, and C. Cerli (2013), Molecular trickery in soil organic matter: Hidden lignin, *Environ. Sci. Technol.*, *47*(16), 9077–9085, doi:10.1021/es401019n.

- Hood, E., and D. Scott (2008), Riverine organic matter and nutrients in southeast Alaska affected by glacial coverage, *Nat. Geosci.*, *1*(9), 583–587, doi:10.1038/ngeo280.
- Johnson, M. S., J. Lehmann, E. G. Couto, J. P. N. Filho, and S. J. Riha (2006), DOC and DIC in flowpaths of Amazonian headwater catchments with hydrologically contrasting soils, *Biogeochemistry*, *81*(1), 45–57, doi:10.1007/s10533-006-9029-3.
- Johnson, M. S., J. Lehmann, S. J. Riha, A. V. Krusche, J. E. Richey, J. P. H. B. Ometto, and E. G. Couto (2008), CO₂ efflux from Amazonian headwater streams represents a significant fate for deep soil respiration, *Geophys. Res. Lett.*, *35*, L17401, doi:10.1029/2008GL034619.
- Koenig, R. (2008), Critical time for African rainforests, *Science*, *320*, 1439–1441.
- Laporte, N. T., J. A. Stabach, R. Grosch, T. S. Lin, and S. J. Goetz (2007), Expansion of industrial logging in Central Africa, *Science*, *316*(5830), 1451–1451, doi:10.1126/science.1141057.
- Laraque, A., J. P. Bricquet, A. Pandi, and J. C. Olivry (2009), A review of material transport by the Congo River and its tributaries, *Hydrol. Process.*, *23*(22), 3216–3224, doi:10.1002/hyp.7395.
- Mann, P. J., A. Davydova, N. Zimov, R. G. M. Spencer, S. Davydov, E. Bulygina, S. Zimov, and R. M. Holmes (2012), Controls on the composition and lability of dissolved organic matter in Siberia's Kolyma River basin, *J. Geophys. Res.*, *117*, G01028, doi:10.1029/2011JG001798.
- Mayorga, E., A. K. Aufdenkampe, C. A. Masiello, A. V. Krusche, J. I. Hedges, P. D. Quay, J. E. Richey, and T. A. Brown (2005), Young organic matter as a source of carbon dioxide outgassing from Amazonian Rivers, *Nature*, *436*(7050), 538–541, doi:10.1038/nature03880.
- Mayorga, E., S. P. Seitzinger, J. A. Harrison, E. Dumont, A. H. W. Beusen, A. F. Bouwman, B. M. Fekete, C. Kroeze, and G. Van Drecht (2010), Global Nutrient Export from WaterSheds 2 (NEWS 2): Model development and implementation, *Environ. Modell. Software*, *25*(7), 837–853, doi:10.1016/j.envsoft.2010.01.007.
- McKnight, D. M., E. W. Boyer, P. K. Westerhoff, P. T. Doran, T. Kulbe, and D. T. Andersen (2001), Spectrofluorometric characterization of dissolved organic matter for indication of precursor organic material and aromaticity, *Limnol. Oceanogr.*, *46*(1), 1–11.
- Mladenov, N., D. M. McKnight, S. A. Macko, M. Norris, R. M. Cory, and L. Ramberg (2007), Chemical characterization of DOM in channels of a seasonal wetland, *Aquat. Sci. Res. Across Boundaries*, *69*(4), 456–471, doi:10.1007/s00027-007-0905-2.
- O'Donnell, J. A., G. R. Aiken, E. S. Kane, and J. B. Jones (2010), Source water controls on the character and origin of dissolved organic matter in streams of the Yukon River basin, Alaska, *J. Geophys. Res.*, *115*, G03025, doi:10.1029/2009JG001153.
- ORSTOM (1979), Mesure des débits à partir des vitesses, *Report. ISBN 2-7099-0546-9*, Office de la Recherche Scientifique et Technique, Paris, France.
- Pellerin, B. A., P. J. Hernes, J. Saraceno, R. G. M. Spencer, and B. A. Bergamaschi (2010), Microbial degradation of plant leachate alters lignin phenols and trihalomethane precursors, *J. Environ. Qual.*, *39*(3), 946–954, doi:10.2134/jeq2009.0487.
- Pellerin, B. A., J. F. Saraceno, J. B. Shanley, S. D. Sebestyen, G. R. Aiken, W. M. Wollheim, and B. A. Bergamaschi (2011), Taking the pulse of snowmelt: In situ sensors reveal seasonal, event and diurnal patterns of nitrate and dissolved organic matter variability in an upland forest stream, *Biogeochemistry*, *108*(1–3), 183–198, doi:10.1007/s10533-011-9589-8.
- Pierrot, D., E. Lewis, and D. W. R. Wallace (2006), MS Excel program developed for CO₂ system calculations, doi:10.3334/CDIAC/otg.CO2SYS_XLS_CDIAC105a.
- Pinney, M. L., P. K. Westerhoff, and L. Baker (2000), Transformations in dissolved organic carbon through constructed wetlands, *Water Res.*, *34*(6), 1897–1911.
- Richey, J. E., J. I. Hedges, A. H. Devol, P. D. Quay, R. Victoria, L. Martinelli, and B. R. Forsberg (1990), Biogeochemistry of carbon in the Amazon River, *Limnol. Oceanogr.*, *35*(2), 352–371.
- Richey, J. E., J. M. Melack, A. K. Aufdenkampe, V. M. Ballester, and L. L. Hess (2002), Outgassing from Amazonian Rivers and wetlands as a large tropical source of atmospheric CO, *Nature*, *416*(6881), 617–620, doi:10.1038/416617a.
- Richey, J. E., A. V. Krusche, M. S. Johnson, H. B. da Cunha, and M. V. Ballester (2009), The role of rivers in the regional carbon balance, in *Amazonia and Global Change, Geophysical Monograph Series*, vol. 186, pp. 489–504, AGU, Washington, D. C., doi:10.1029/2008GM000734.
- Sanderman, J., K. A. Lohse, J. A. Baldock, and R. Amundson (2009), Linking soils and streams: Sources and chemistry of dissolved organic matter in a small coastal watershed, *Water Resour. Res.*, *45*, W03418, doi:10.1029/2008WR006977.
- Spencer, R. G. M., G. R. Aiken, K. P. Wickland, R. G. Striegl, and P. J. Hernes (2008), Seasonal and spatial variability in dissolved organic matter quantity and composition from the Yukon River basin, Alaska, *Global Biogeochem. Cycles*, *22*, GB4002, doi:10.1029/2008GB003231.
- Spencer, R. G. M., et al. (2009), Photochemical degradation of dissolved organic matter and dissolved lignin phenols from the Congo River, *J. Geophys. Res.*, *114*, G03010, doi:10.1029/2009JG000968.
- Spencer, R. G. M., G. R. Aiken, R. Y. Dyda, K. D. Butler, B. A. Bergamaschi, and P. J. Hernes (2010a), Comparison of XAD with other dissolved lignin isolation techniques and a compilation of analytical improvements for the analysis of lignin in aquatic settings, *Org. Geochem.*, *41*(5), 445–453, doi:10.1016/j.orggeochem.2010.02.004.
- Spencer, R. G. M., P. J. Hernes, R. Ruf, A. Baker, R. Y. Dyda, A. Stubbins, and J. Six (2010b), Temporal controls on dissolved organic matter and lignin biogeochemistry in a pristine tropical river, Democratic Republic of Congo, *J. Geophys. Res.*, *115*, G03013, doi:10.1029/2009JG001180.
- Spencer, R. G. M., et al. (2012a), An initial investigation into the organic matter biogeochemistry of the Congo River, *Geochim. Cosmochim. Acta*, *84*(0), 614–627, doi: 10.1016/j.gca.2012.01.013.
- Spencer, R. G. M., K. D. Butler, and G. R. Aiken (2012b), Dissolved organic carbon and chromophoric dissolved organic matter properties of rivers in the USA, *J. Geophys. Res.*, *117*, G03001, doi:10.1029/2011JG001928.
- Spencer, R. G. M., G. R. Aiken, M. M. Dornblaser, K. D. Butler, R. M. Holmes, G. Fiske, P. J. Mann, and A. Stubbins (2013), Chromophoric dissolved organic matter export from U.S. rivers, *Geophys. Res. Lett.*, *40*, 1575–1579, doi:10.1002/grl.50357.
- Spencer, R. G. M., A. Stubbins, and J. Gaillardet (2014), Geochemistry of the Congo River, estuary and plume, in *Biogeochemical Dynamics at Large River-Coastal Interfaces: Linkages With Global Climate Change*, edited by T. S. Bianchi, M. A. Allison, and W. J. Cai, pp. 554–584, Cambridge Univ. Press, Cambridge, U. K.
- Striegl, R. G., G. R. Aiken, M. M. Dornblaser, P. A. Raymond, and K. P. Wickland (2005), A decrease in discharge-normalized DOC export by the Yukon River during summer through autumn, *Geophys. Res. Lett.*, *32*, L21413, doi:10.1029/2005GL024413.
- U.S. Environmental Protection Agency (1984), Methods for chemical analysis of water and wastes, Rep. EPA-600/4-79-020, Washington, D. C.
- U.S. Geological Survey (2000), HYDRO1K elevation derivative database, Cent. for Earth Resour. Obs. and Sci., Sioux Falls, S.D, <http://edc.usgs.gov/products/elevation/gtopo30/hydro>.
- Wang, Z. A., and W.-J. Cai (2004), Carbon dioxide degassing and inorganic carbon export from a marsh-dominated estuary (The Duplin River): A marsh CO₂ pump, *Limnol. Oceanogr.*, *49*, 341–354.
- Wang, Z. A., D. J. Bienvenu, P. J. Mann, K. Hoering, J. Poulsen, R. G. M. Spencer, and R. M. Holmes (2013), Inorganic carbon speciation and fluxes in the Congo River, *Geophys. Res. Lett.*, *40*, 511–516, doi:10.1002/grl.50160.

- Ward, N. D., R. G. Keil, P. M. Medeiros, D. C. Brito, A. C. Cunha, T. Dittmar, P. L. Yager, A. V. Krusche, and J. E. Richey (2013), Degradation of terrestrially derived macromolecules in the Amazon River, *Nat. Geosci.*, *6*(6), 1–4, doi:10.1038/ngeo1817.
- Weishaar, J. L., G. R. Aiken, B. A. Bergamaschi, M. S. Fram, R. Fujii, and K. Mopper (2003), Evaluation of specific ultraviolet absorbance as an indicator of the chemical composition and reactivity of dissolved organic carbon, *Environ. Sci. Technol.*, *37*(20), 4702–4708, doi:10.1021/es030360x.
- Weiss, R. F. (1974), Carbon dioxide in water and seawater: The solubility of a non-ideal gas, *Mar. Chem.*, *2*, 203–215.
- Wilson, H. F., and M. A. Xenopoulos (2008), Ecosystem and seasonal control of stream dissolved organic carbon along a gradient of land use, *Ecosystems*, *11*(4), 555–568, doi:10.1007/s10021-008-9142-3.
- Worrall, F., H. Davies, A. Bhogal, A. Lilly, M. Evans, K. Turner, T. Burt, D. Barraclough, P. Smith, and G. Merrington (2012), The flux of DOC from the UK—Predicting the role of soils, land use and net watershed losses, *J. Hydrol.*, *448–449*(C), 149–160, doi:10.1016/j.jhydrol.2012.04.053.
- Yamashita, Y., N. Maie, H. Briceño, and R. Jaffé (2010), Optical characterization of dissolved organic matter in tropical rivers of the Guayana Shield, Venezuela, *J. Geophys. Res.*, *115*, G00F10, doi:10.1029/2009JG000987.
- Yamashita, Y., B. D. Kloeppel, J. Knoepp, G. L. Zausen, and R. Jaffe (2011), Effects of watershed history on dissolved organic matter characteristics in headwater streams, *Ecosystems*, *14*, 1110–1122, doi:10.1007/s10021-011-9469-z.